A PROTOTYPE DIPOLE SEPTUM MAGNET FOR FAST HIGH CURRENT KICKER SYSTEMS*

L. Wang[1], S. M. Lund, G. J. Caporaso, Y. J. (Judy) Chen, B. R. Poole, LLNL, Livermore, CA
T. F. Brown, Bechtel Nevada Corporation, Las Vegas, NV

Abstract

A dipole "septum" magnet without a material septum has been designed and tested as part of a fast beam kicker system for use in intense, electron-beam induction accelerators. This septum magnet is a simple, iron-based electromagnet with two static, oppositely oriented dipole field regions used to provide further separation of beam centroids given a small angle kick by a fast beam kicker. The magnet geometry includes removable pole pieces to allow experimental flexibility. Field errors experienced by the beam depend crucially on the magnitude of the initial kick that provides displacement of the beam centroids from the transition region between the two dipole field regions. Results of simulations are reported.

1 INTRODUCTION

Intense electron-beam induction accelerators are presently under consideration at Lawrence Livermore National Laboratory (LLNL) for use in advanced flash x-ray diagnostics of implosions [1]. A key component of these radiography machines is a fast, high current stripline kicker used to rapidly switch an intense electron beam micro-pulse on the order of 50 ns in duration into separate beam transport lines to achieve multiple lines of sight on target [2]. This fast kicker system is composed of two elements in series as diagrammed in Fig. 1. The first is a fast dipole kicker that is only capable of imparting a small angle bend ($\theta_i \approx 1^o$) to the centroid. This is followed by a short drift distance to allow the kicked beam centroids to radially separate (but not so long as to allow significant expansion due to the lack of transverse focusing), and then a static field dipole septum magnet that increases the angular separation of the centroids ($\theta_f \approx 15^o$) and steers them into separate transport lines. In this study, we describe the design and construction of a prototype septum magnet with two oppositely oriented dipole field regions. This "septum" magnet is not a true septum since no material is allowed in the region between the two dipole field apertures across which intense electrons will spray during the beam switching process. Any material present in this region would be hit by intense electrons and resulting plasmas close to the beam reference orbits could interfere with subsequent micro-pulses. Unfortunately, this lack of a material septum makes achieving high field quality problematic. A simple, flexible iron-dominated dipole electromagnet has been designed for use in proof-of-principle experiments on the ETA-II accelerator at LLNL. This design scales to full radiographic parameters, and allows a wide range of experimental tuneability.

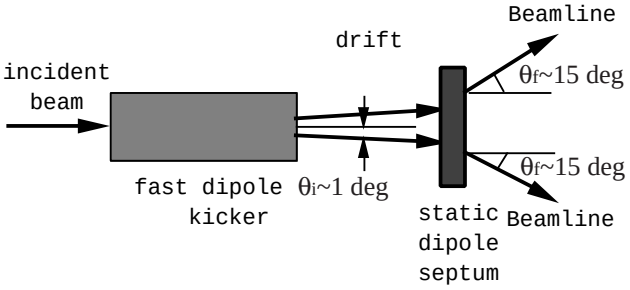

Fig. 1: Fast kicker system consisting of a pulsed, fast dipole kicker, a drift, and a static dipole septum magnet.

The ideal "box" geometry of the septum magnet is shown in Figure 2. There are two regions with oppositely oriented uniform, dipole magnetic fields of the same magnitude, radially separated by a thin field transition region. The two beams emerging from the kicker are incident in the uniform field region a radial distance d from the centerline and are further separated from each other by the dipole fields as the beams traverse the axial length l of the magnet.

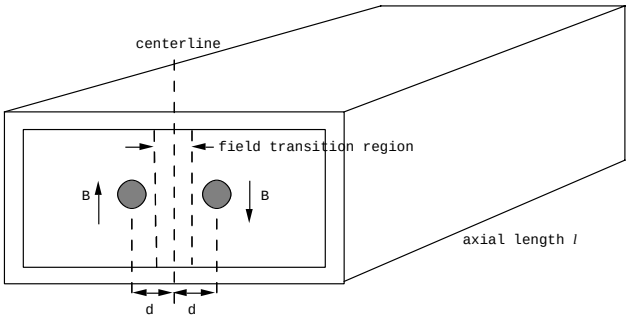

Fig. 2: Ideal box geometry of the dipole septum magnet.

The required dipole magnetic field B is related to the beam energy E_b and the incident and exiting beam angles θ_i and θ_f by

$$Bl = \frac{mc}{e}\sqrt{\left(\frac{E_b}{mc^2}\right)^2 + 2\left(\frac{E_b}{mc^2}\right)}\left[\sin\theta_f - \sin\theta_i\right] . \qquad (1)$$

*The work was performed under the auspices of the U. S. Department of Energy under contract W-7405-ENG-48.

[1] Email: wang22@llnl.gov

Here, m and e are the mass and charge of an electron, and c is the speed of light in vacuo. On traversing the magnet, the beam centroids will move radially a distance

$$\Delta = l\frac{\left[\cos\theta_i - \cos\theta_f\right]}{\left[\sin\theta_f - \sin\theta_i\right]} \quad . \qquad (2)$$

2 SEPTUM MAGNET DESIGN

An iron electromagnet has been designed using iron poles with shims to enhance field quality. The magnet geometry is illustrated in Fig. 3 and is essentially two "C" type dipole magnets brought into close radial proximity. The poles consist of insertable plates allowing easy pole replacement enabling experimental evaluation of a range of aperture gaps, and field smoothing shims using the same basic assembly. The rapidity of the transition between the two dipole field regions depends critically on h/d, the ratio of magnet half-gap h relative to the incident centroid displacement d. The ratio d/r_b, where r_b is the beam radius, must also be sufficiently large such that the incident beam does not enter the field transition region. Achievable d is limited by the fast kicker technology and the maximum fast-kicker to septum magnet drift distance. Thus h was chosen as small as possible consistent with the transverse size of the nearly round beam incident on the septum magnet. The dipole fields bend the beam centroid into the good field region as the beam traverses the box magnet geometry. Due to this desire to increase the centroid motion Δ [Eq. (2)] and the desire to minimize 3D fringe field effects, weak bending fields were employed with long axial magnet length relative to the magnet half-gap h. Coils were stacked thin transversely and long vertically to allow a more rapid transition between the dipole field regions. Permanent magnets and/or additional coils could be used to enhance the rapidity of the field transition, but this was avoided for simplicity and to have the unsaturated field scale linearly with coil excitation. The upper and lower half coils were wound separately to allow the upper and lower magnet assemblies to be unbolted for easy removal of the magnet assembly and independent excitation of each dipole region. This allows easy access to the poles and the vacuum beam pipe as well as flexible experimental operation. Shims were employed near the field transition region to enhance field linearity. The vertical height of these shims was limited to prevent further restriction of a thin walled rectangular vacuum pipe that threads the magnet aperture, thereby limiting the degree of field smoothing these shims can produce. No shims were employed on the far radial extent of the poles since the poles can easily be made wide enough to achieve high field quality in that region.

The parameters chosen for the design are an axial length $l = 20\,\text{cm}$, incident and exiting beam angles of $\theta_i = 1\,\text{deg}$ and $\theta_f = 15\,\text{deg}$, resulting in a bending field of $B \approx 250\,\text{Gauss}$ for the beam energy of $E_b \approx 6\,\text{MeV}$. The incident beam radius (r_b) and centroid separation ($2d$) at the septum magnet are about 1.5 cm and 6 cm, respectively. The beam centroid will exit the magnet a horizontal distance of $\Delta \sim 3\text{cm}$.

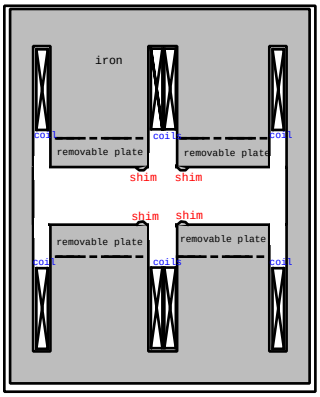

Fig. 3: Schematic of dipole septum magnet geometry (not to scale).

Figure 3 shows the 2D geometry of the septum magnet designed. The beams go through the aperture ($2h$) which is about 7 cm high. The coils on the left side and right side of the magnet have different polarities such that there are two field regions with oppositely oriented dipole magnetic fields. The amp-turns of each coil can be estimated as $NI \approx Bh/\mu_0 \sim 800$ Amp-turns. Here, h is the height of the half gap, μ_0 is the free space permittivity, and N is the number of turns of the coil. A total of $N = 300$ turns was chosen and the total power dissipation was small enough where no water cooling was needed. A part of each iron pole is made into a removable plate. Therefore, if the beam radius is larger than expected or if the field quality is insufficient, the gap structure can be easily modified without reconstructing the whole magnet assembly. Shims of trapezoidal shape were designed to make the fields more uniform in the transition region. A picture of the septum magnet built for use in proof-of-principle experiments on the ETA-II accelerator at LLNL is displayed in Fig. 4a. Figure 4b shows the septum magnet in the beamline. Because of the small aperture in the septum magnet, the round beam pipe from the kicker is tapered to a rectangular shape in the septum magnet region before reaching the diverging beamline.

(a) (b)

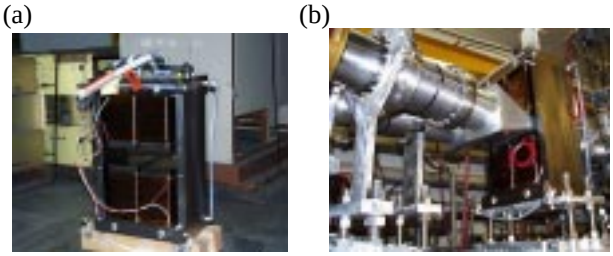

Fig. 4: (a) Septum magnet for the ETA-II experiment
(b) Septum magnet in the beamline

3 MAGNETIC FIELD SIMULATION

The magnetic field was simulated using the 2D magnetostatic code Poisson. Only a quarter of the symmetric structure was simulated. Due to the low fields, no iron saturation occurred for the full possible coil excitation. Figures 5a and 5b show the field contours near the transition region without and with the shims. The curved field lines indicate non-uniform fields, with a perfect dipole corresponding to straight lines.

(a)

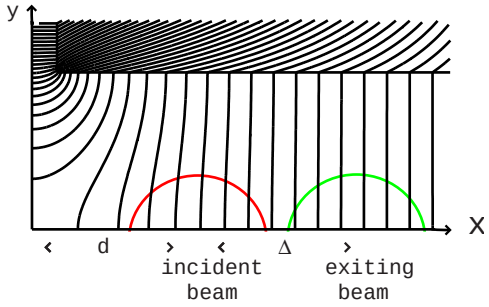

(b)

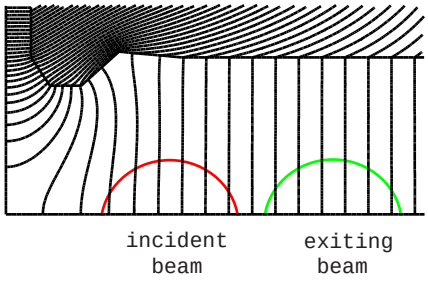

Figure 5: Simulated field lines in the half aperture of the septum magnet. (a) without shims. (b) with shims.

Note that with shims, the fields in the transition region are more uniform. Also the significant centroid motion of the beam from incident to exiting limits the effect of the larger incident field errors since the beam bends into the high field quality region. Note also that the shim includes a small tapered cut from the iron pole. The effect of the shim is further illustrated in Fig. 6, where the vertical magnetic field on the midplane ($y = 0$) of the septum magnet is plotted. Note that the shim reduces the undesirable variation in field at the beam edge and centroid for the incident beam.

A harmonic analysis of the multipole content of the field in the gap of was performed at x=3, 4, 5, and 6 cm and $y = 0$. Table 1 summarizes the multipole field contributions compared to the dipole field at that value of x when evaluated on a circle of radius 2.5 cm for harmonic numbers $N = 2$ (quadrupole), 3 (sextupole), and 4 (octupole).

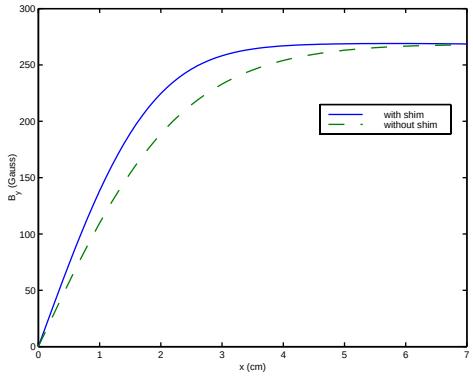

Figure 6: Vertical magnetic field on the midplane of the septum magnet verses radial distance from magnet center.

Table 1: Harmonic analysis of the field inside the aperture

N	x= 3cm	x=4cm	x=5cm	x=6cm
2	6.5%	1.4%	0.3%	0.04%
3	4.5%	1.1%	0.2%	0.1%
4	1.8%	0.6%	0.1%	0.00%

4 EMITTANCE CALCULATION

To estimate emittance growth in the magnet due to the field non-uniformity, a 3D PIC simulation was used to transport a uniform beam slice consisting of several thousand particles through the magnet [3]. The trajectories were calculated either by using an analytic approximation for the fields or by importing the 2D field map from Poisson simulations. Preliminary estimates show emittance growth on the order of 4% for the magnet, which is acceptable in the experiment.

5 CONCLUSION

An electromagnet septum magnet was designed and fabricated for experiments on the ETA-II accelerator. This design avoided the use of a material septum and was based on a simple scaleable geometry which allows a high degree of experimental flexibility. The device is in use in experiments. Results of more detailed measurements and experimental field map comparisons will be reported in future work.

6 REFERENCES

[1] G. J. Caporaso, in the Proc. of the Joint US-CERN-Japan International School, Maui, Hawaii, USA, November 3-9, 1994, edited by S. I. Kurokawa, M. Month, S. Turner, pp 594-615, (1996).

[2] Y. J. (Judy) Chen, G. J. Caporaso, J. T. Weir, "Precision Fast Kickers for Kiloampere Electron Beams", 1999 Particle Accelerator Conference, New York, New York, USA, March 29 - April 2, (1999).

[3] B. R. Poole, G. J. Caporaso, Y. J. (Judy) Chen, L.-F. Wang, "Analysis and Modeling of a Stripline Beam Kicker and Septum", XIX International Linac Conference, Chicago, IL, USA, August 23-28, (1998), LLNL UCRL-JC-130414.